

A Robust Object Encoding Method

Kuan Xu^{†1}, Chen Wang^{†2}, Chao Chen¹, and Wei Wu¹

Abstract—Object encoding and identification is crucial for many robotic tasks such as autonomous exploration and semantic relocalization. Existing works heavily rely on the tracking of detected objects but difficult to recall revisited objects precisely. In this paper, we propose a novel object encoding method based on a graph of key-points. To be robust to the number of key-points detected, we propose a feature sparse encoding and object dense encoding method to ensure that each key-point can only affect a small part of the object descriptors, leading it robust to viewpoint changes, scaling, occlusion, and even object deformation. In the experiments, we show that it achieves superior performance for object identification than the state-of-the-art algorithm and is able to provide reliable semantic relocalization. It is a plug-and-play module and we expect that it will play an important role in the robotic applications.

I. INTRODUCTION

Object encoding and identification is of great importance for many robotic tasks such as autonomous exploration and semantic re-localization in simultaneous localization and mapping (SLAM). For example, in autonomous exploration, an efficient and robust object encoding benefits the decision process when a robot revisits a specific landmark object [1]. Without the capability of object re-identification, a semantic SLAM system may easily drift and subsequently leads to an unreliable localization [2]. However, existing object encoding methods easily produce false matches due to viewpoint or scaling changes, hence a robust and efficient object encoding method is necessary for many robotic applications.

To save computational resources, object matching in SLAM is often based on key-point features [3], as the feature-based SLAM [4] is still the most widely used method. Inspired by the recent progresses in deep learning-based key-point detector [5] and feature matcher [6], it becomes intuitive to encode an object via a group of detected key-points in an end-to-end way, where the key-points on the same object forms a graph neural network. Therefore, we can take the graph embedding as the object descriptors.

However, this is not straightforward and very difficult, since the number of detected object key-points are affected by many factors such as illumination and object deformation. Moreover, during robot exploration, robots often observe part of the objects due to occlusion and different viewpoint, resulting in that the object key-points only has a small overlap across different frames. Therefore, the key-points graph embedding will also be easily affected, which makes it difficult to directly

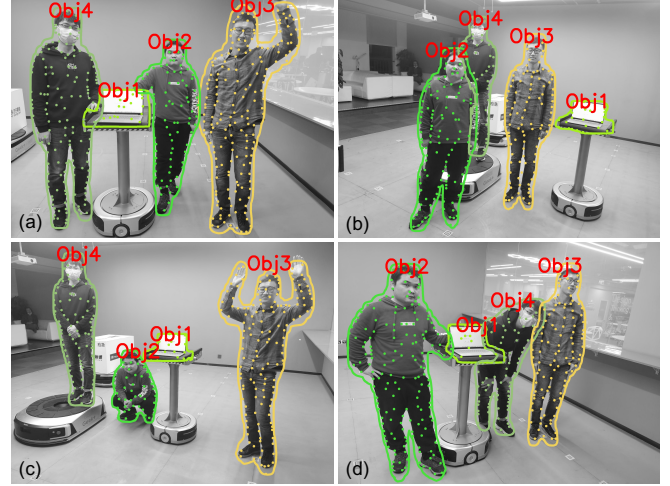


Fig. 1: A live object matching demo. Four objects including 1 rigid object and 3 non-rigid objects (human) are identified. Our proposed encoding method is insensitive to viewpoint (Obj 1 in (b) and (d)), scaling (Obj 3 and Obj 4), occlusion (Obj 4), and even posture change (Obj 2 and Obj 3).

apply a graph model [7]. To solve this problem, we argue that a key-point descriptor should have a sparse effect on the object embedding. This means that only a few positions of an object descriptor can be affected if a key-point is added or removed from an object graph. To achieve this, we propose a sparse object encoding method, which makes the object descriptors robust to viewpoint changes and deformation.

In summary, the main contributions of this paper are

- We introduce a simple yet effective pipeline for robust object encoding and present a plug-and-play sparsity layer, where similar sparse key-points are clustered.
- We propose sparse loss for key-point features and dense loss for object features to ensure the object encoder insensitive to the appearance of specific feature points.
- Our method provides reliable object matching as shown in Fig. 1 and we demonstrate its effectiveness in semantic relocalization compared to the state-of-the-art method.

II. RELATED WORK

In this section, we will review both object encoding and visual place recognition methods, since some place recognition algorithms can also be applied to object identification. Although proposed early, feature matching is still the most popular strategy for object re-identification due to its efficiency, especially in robotic applications. Descriptors from networks such as Mask R-CNN [8] will not be included,

[†]Kuan Xu and Chen Wang contribute equally.

¹Kuan Xu, Chao Chen, and Wei Wu are with the Geek+ Corp. {xukuan, chenchao, merlinwu}@geekplus.com

²Chen Wang is with the Robotics Institute, Carnegie Mellon University, Pittsburgh, PA 15213, USA. chenwang@dr.cmu.edu

since they are designed for general objects detection and difficult to be used for re-identification.

A. Handcrafted Feature-based Methods

One of the most classic approaches based on handcrafted features is the fast appearance-based mapping (FABMAP) [9]. In FABMAP, the visual vocabulary of SURF feature [10] is trained by hierarchical k-means clustering to discretize its high dimensional representation. Revisited objects are then identified by matching feature distribution over the offline trained visual vocabulary. Similar idea is employed in DBoW2 [11], in which the binary descriptor ORB [12] is used instead. It achieves faster speed due to the binary feature representation. Emilio *et al.* [13] introduce a vocabulary maintenance strategy called dynamic island that groups similar images. It is able to identify repetitive registration of same descriptor across multiple frames. The database is kept at a small scale by removing redundant descriptors.

Schlegel *et al.* [14] introduce an online trained Hamming distance embedded binary search tree (HBST) for image retrieval which is much faster than traditional FLANN matching methods. However, the memory cost is huge since raw descriptors are used to build the incremental visual vocabulary tree. Applying dimensional reduction on local features is also an alternative solution. Carrasco *et al.* [15] adopt the idea from image encoding to extract local descriptors. Hash coding is applied to the local features array collected from single image so that the extracted features are more compact. Gehrig *et al.* [16] directly apply principle component analysis (PCA) for BRISK [17] feature. Instead of searching on pre-trained visual vocabulary, k-nearest neighbor (K-NN) search is performed on the projected descriptors that achieves faster speed at the level of millisecond for each query. However, those methods require handcrafted feature extraction, which is sensitive to environment changes.

Tsintotas *et al.* [18] adopt a dynamic quantization strategy to train the feature online, in which a growing neural gas [19] network is applied. To utilize both structural and visual information, Stumm *et al.* introduce covisibility graph to represent visual observations [20]. To jointly consider external information, Schlegel *et al.* embed continuous and selector cues by augmenting each feature descriptor with a binary string [21]. Although widely-used, the feature-based methods performs not well when the descriptors are not discriminative enough, *e.g.* when the visual texture is similar, hence we argue that an object-level place recognition is necessary.

B. Deep Feature-based Methods

The recent success of convolutional neural network (CNN) in computer vision [22] has triggered another research trend. For example, in [23], a multi-scale feature encoding method is introduced by training two CNN architectures. The generated CNN features are viewpoint invariant, hence a large performance improvement is achieved. Inspired by the traditional image retrieval method, *i.e.*, vector of locally aggregated descriptors (VLAD), Relja *et al.* propose the NetVLAD [24] to learn CNN parameters in an end-to-end

manner. Hausler *et al.* [25] combine both feature-based methods and the CNN techniques. The query image is trained by combining sum of absolute difference (SAD), histogram of oriented gradients (HOG) [26], CNN spatial Max pooling and CNN spatial Arg-Max pooling.

To overcome the problem of training data deficiency and multi-modality input dissimilarity, an RGB-D object recognition framework is proposed to effectively embed depth and point cloud data into the RGB domain [27]. Zaki *et al.* incorporate depth information into a transferred CNN model from image recognition by rendering objects from a canonical perspective and colorizing the depth channel according to distance from the object center [28]. HP-CNN [29] presents a multi-scale object feature representation based on a multi-view 3D object pose using RGB-D sensors.

Our object encoding method is established on deep feature points and descriptors, which received increasing attentions recently. For example, SuperPoint [5] proposed a self-supervised framework for training interest point detectors and descriptors. SuperGlue [6] introduced a graph attention model into SuperPoint for feature matching. Intuitively, the interest point and their descriptors form a large temporal growing graph, in which the feature points are nodes, and their associated descriptors are the node features.

III. METHODOLOGY

A. Motivation

Inspired by the fact that human can easily identify an object by recognizing both local distinctive features and global structure [30], we argue that a robust object encoding method should have the following properties: (1) An object descriptor should be able to encode its key-point descriptors located on it; (2) The object descriptor should also contain the global or semi-global structural information; (3) To overcome viewpoint changes or deformation, the object descriptor should be insensitive to the existence of the key-points on it.

The above properties indicate that an object descriptor should be dependent on the local feature points but only specific elements can be affected by one key-point. In another word, a key-point descriptor has a sparse effect on the object descriptor. This inspires us to formulate the object encoding as a problem of graph sparse embedding, in which the nodes are key-points, while the edges are the point connections.

B. Formulation

Given a group of feature points from the same object, each of which is denoted as position $\mathbf{p}_i = (x, y)$, $i \in [1, M]$ and associated visual descriptor $\mathbf{d}_i \in \mathbb{R}^{N_p}$, where N_p is the dimension of the key-point descriptor. Our goal is to design a graph neural network to generate an object descriptor $\mathbf{D}_k \in \mathbb{R}^{N_o}$, where $N_o > N_p$ is the dimension of the object descriptor, based on a group of feature points detected on that object.

Therefore, we propose a simple yet effective pipeline for object matching in Fig. 2, where each object is taken as a graph, where the nodes are the points \mathbf{p}_i and node features are \mathbf{d}_i . In practice, they are obtained from object segmentation mask from pretrained Mask R-CNN [8] and point detector

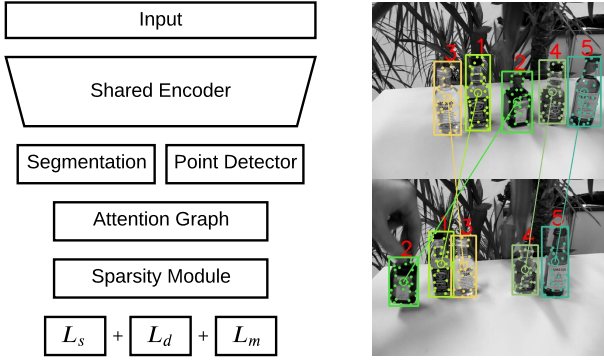


Fig. 2: The network structure of our object encoding method and an example of object matching from the OTB dataset.

SuperPoint [5], where a backbone encoder VGG-16 [31] is shared. Therefore, we are able to obtain the key-point descriptors, which are grouped by their associated object labels from the segmentation header. The grouped key-point descriptors are then taken as the input of a two-layer attention graph module [32], which will allow the key-point embedding explicitly encoding the object structural information, which will be presented in Section III-C.1. Afterwards, this key-point node embedding which contains both structural and local information will decide their sparse locations on the object descriptor via learned location feature, which will be shown in Section III-C.2. Finally, the network is supervised by the sparse, dense, and matching loss, which will be presented in Section III-C.3, III-C.4, and III-C.5, respectively.

This work can also be built on handcrafted descriptors such as SIFT [33]. We note that an attention graph is also used in SuperGlue [6] to match the feature points, while our objective is to generate object descriptor. Moreover, SuperGlue broadcasts node features from two images for point matching, while we argue that the object embedding should be self-representative thus the node features can only be propagated within the object. This is because we expect that an object descriptor doesn't use information from external images, so that one query descriptor can be matched to objects in database without exchanging information. We next present the proposed sparsity module and loss functions, respectively.

C. Graph Embedding with Sparse Node Features

1) *Node Encoding*: Different from SuperGlue that encodes node features in the first graph layer as a summation of the point descriptor and a transform of point position, we instead encode node features \mathbf{x}_i as their concatenation:

$$\mathbf{x}_i^{(1)} = [\mathbf{d}_i || \text{MLP}(\mathbf{p}_i)], \quad \mathbf{x}_i \in \mathbb{R}^{N_n}, \quad (1)$$

where $N_n = N_p + N_m$, $||$ is the concatenation operator, $\text{MLP}: \mathbb{R}^2 \mapsto \mathbb{R}^{N_m}$ is a multi-layer perceptron module, and the superscript of $\mathbf{x}_i^{(l)}$ denote the l -th layer. In practice, the position \mathbf{p}_i is normalized to $[-1, 1]$ by the object size, which takes the object center as the origin. The concatenation operator is vital for the (2) and (3) properties mentioned in Section III-A: This is because that (a) It is helpful for

explicitly learning the object structure, as the relative position information will not blended into the descriptor and (b) The sparse non-zero locations will be able to learn from the object structure, which will be further explained in Section III-C.2.

2) *Sparsity Layer*: Inspired by the (3) property mentioned in Section III-A, we argue that a key-point descriptor should only be able to affect the object descriptor on sparse locations, so that the key-points can be added or removed without significantly changing the object descriptor. Moreover, to fully utilize the expressive power of the object descriptor, which is often much longer than point descriptor, key-points with different local patterns should be written into distinctive locations. Therefore, the sparse locations should be learned from the contents of the key-point descriptor. To achieve this, we define the sparsity layer in (2) for the location node feature and content node feature.

$$^{(l+1)}\mathbf{x}_i^L = \text{ReLU}(\mathbf{W}_L^{(l)} \cdot ^{(l)}\mathbf{x}_i^L), \quad (2a)$$

$$^{(l+1)}\mathbf{x}_i^C = \text{ReLU}(\mathbf{W}_C^{(l)} \cdot ^{(l)}\mathbf{x}_i^C), \quad (2b)$$

where $\mathbf{W}_L^{(l)}, \mathbf{W}_C^{(l)} \in \mathbb{R}^{N_o \times N_n^l}$, $N_n^l < N_o$ are the learnable location and content weights, respectively. We set $^{(1)}\mathbf{x}_i^L = ^{(1)}\mathbf{x}_i^C$ as the output of attention graph and construct two branches, each of which has two layers to learn the location and content features, respectively. If the location feature \mathbf{x}_i^L is a sparse vector that only a few locations are non-zero, an object descriptor \mathbf{D}_k will be insensitive to the change of key-points.

$$\mathbf{D}_k = \frac{\mathbf{W}_O}{M} \sum_{i=1}^M \mathbf{x}_i^L \odot \mathbf{x}_i^C, \quad (3)$$

where \mathbf{W}_O is learnable parameters and the operator \odot is an element-wise multiplication. Note that the summation in (3) is a symmetric operator, which is able to make the object descriptor \mathbf{D}_k invariant to the permutation of key-points.

3) *Sparse Location Loss*: To ensure the sparsity, we define the location sparse loss L_s as the ℓ_1 -norm of \mathbf{x}_i^L .

$$L_s := \sum_{i=1}^M \|\phi(\mathbf{x}_i^L)\|_1, \quad (4)$$

where $\phi(\mathbf{x}) = \mathbf{x}/\|\mathbf{x}\|_2$ is a ℓ_2 -normalization function, which is to prevent the location feature from being zero. Therefore, the location feature \mathbf{x}_i^L tends to approach the axes due to the constraint of the unit length. A more intuitive explanation in 2-D space is that the points located on the intersection of axes and unit circle has the minimum ℓ_1 -norm.

4) *Dense Feature Loss*: The location sparse loss ensures that the key-point descriptors are encoded into sparse locations on the object descriptor. On the other hand, we also expect that distinctive key-point descriptors are able to cover different locations, which can maximize the space utilization rate of the object descriptor, otherwise the location weights \mathbf{W}_L will simply learn to map all key-points to the same sparse locations, which is not expected. Therefore, we define a feature dense loss L_d as the negative ℓ_1 -norm of the location features to improve the density of the object descriptor.

$$L_d := \max \left(0, \delta - \phi \left(\left\| \sum_{i=1}^M \mathbf{x}_i^L \right\|_1 \right) \right), \quad (5)$$

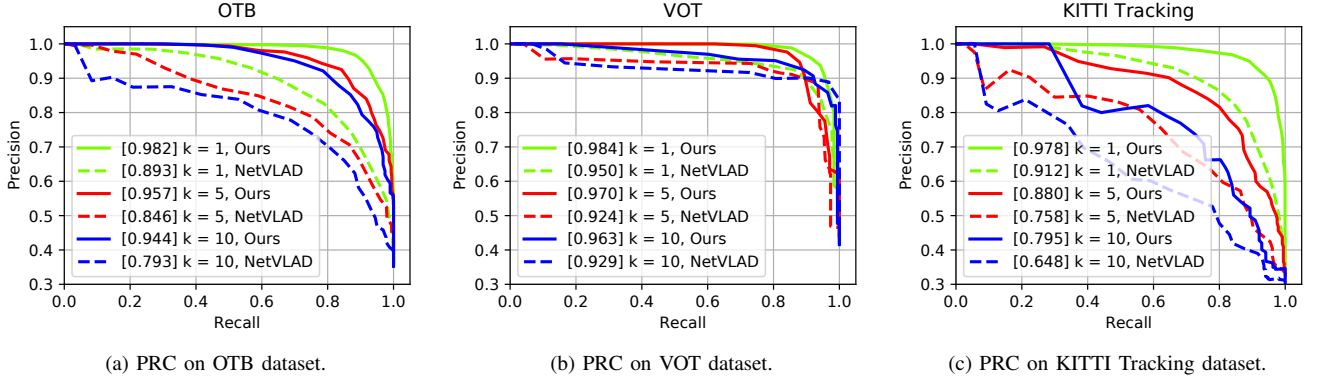


Fig. 3: The precision-recall curves (PRC) on object matching. The area under curves are shown in the [brackets].

where $\delta > 0$ is a positive constant. A major difference of the dense loss (5) from the sparse loss (4) is that the summation operator is inside of the ℓ_1 -norm, while the ℓ_2 -normalization function ϕ is outside of the ℓ_1 -norm. This is because that the object descriptor (3) is an element-wise summation of the key-point features. Intuitively, by optimizing the sparse loss and dense loss simultaneously, we are able to push the key-point location features to be sparse, while retaining the density of object descriptor, so that similar key-points will share similar locations, while distinctive key-points tend to cover different locations. This will make the object descriptor insensitive to the changes of key-points, which is also the key of our viewpoint and deformation invariant object encoding.

Note that the sparsity in this paper is different from the traditional sparse coding techniques [34] and deep sparse coding network [35] which are to learn a dictionary and minimize a reconstruction error, while ours is to learn sparse key-point features without any approximation and dictionary. It is also different from the model compression networks such as [36] to learn sparse convolutional weights, as we have no sparse constraints on the learnable weights \mathbf{W}_L .

5) *Object Matching Loss*: The object matching loss (6) maximizes the cosine similarity for positive object pairs, while minimizes the cosine similarity for negative pairs.

$$L_m := \sum_{\{p,q\} \in P^+} (1 - S(\mathbf{D}_p, \mathbf{D}_q)) + \sum_{\{p,q\} \in P^-} \max(0, S(\mathbf{D}_p, \mathbf{D}_q) - \zeta), \quad (6)$$

where $\zeta = 0.2$, S is the cosine similarity, and P^+ and P^- are positive and negative object matching pairs, respectively.

IV. EXPERIMENTS

A. Implementation Details and Baseline

We take pre-trained backbone CNN and key-point detector from SuperPoint [5], pre-trained segmentation header from Mask R-CNN [8], and finetune the entire network on COCO dataset [37]. Random homographies are generated for data augmentation, including the perspective, translation, rotation, and scale transforms. We take a batch size of 16, a learning

rate of 10^{-5} , and the RMSprop [38] optimizer for training. In the experiments, we set $N_p = 256$, $N_m = 16$, and $N_o = 2048$.

We will perform extensive comparison with one of the state-of-the-art methods, NetVLAD [24]. We mainly compare with NetVLAD because it is also a plug-and-play module and one of the most famous image matching methods. More importantly, it has been adopted by many place recognition algorithms, e.g., [39], [40], which verifies its generalization ability. To be fair, we adopt the same architecture as ours.

B. Object Matching

We first present the performance of the proposed method on object matching. Three datasets will be tested extensively, including OTB [41], VOT [42], and KITTI Tracking [43]. Note that we present performance on tracking datasets but will not compare with object tracking methods such as [44], as tracking is mainly to use the information from consecutive frames, while we aim to extract robust object descriptors for matching with any frames. Note that we don't perform any fine tuning on the three tracking datasets.

1) *OTB Dataset*: We select all sequences of OTB in which objects have labels in the COCO dataset and can be detected by more than 5 key-points. To test the robustness, we report the matching performance for frame pairs that has $k-1$ frames in between. Intuitively, matching is more difficult for larger k and we have $k=1$ for object tracking. We take an object pair as a match if their cosine similarity is larger than a threshold δ . The overall performance of precision, recall, and F1-score is presented in Table I. It can be seen that our method outperforms NetVLAD with a large margin of 5%-15%. Intuitively, if we change the threshold δ , we can obtain the precision-recall curves (PRC) for each sequence. We report the precision-recall curves in Fig. 3a, in which the area under curves (PRC) are also reported in the brackets. Our method achieves a much higher performance for all cases, i.e., an average higher performance of 8.9%, 11.1%, and 15.1% for $k=1, 3$, and 10, respectively. We notice that the performance of our method decreases much slower with increasing k , which verifies its robustness.

2) *VOT Dataset*: We next perform similar evaluation on the VOT dataset, which mainly contains blur and non-rigid



Fig. 4: The examples of car matching in the KITTI Odometry dataset. Although all the cars look similar, our method is still able to correctly identify the same cars from different viewpoint.

TABLE I: Object Matching on the OTB dataset.

	Method	Precision	Recall	F1
$k = 1$	NetVLAD	78.5	83.0	80.7
	Ours	92.7	92.6	92.6
$k = 3$	NetVLAD	72.7	79.7	76.0
	Ours	88.0	85.3	86.6
$k = 5$	NetVLAD	74.0	81.0	77.3
	Ours	87.0	87.9	87.4
$k = 10$	NetVLAD	70.2	80.7	75.1
	Ours	85.2	86.9	86.0

objects such as human. The overall performance is presented in Table II, in which we achieve an higher performance of 1-5%. The PRC performance is further reported in Fig. 3b, in which we achieve a higher performance of 3.4%, 4.6%, and 3.4%, for $k = 1, 5$, and 10 , respectively.

TABLE II: Object Matching on the VOT dataset.

	Method	Precision	Recall	F1
$k = 1$	NetVLAD	90.9	88.7	89.8
	Ours	96.0	91.3	93.6
$k = 3$	NetVLAD	90.0	92.1	91.0
	Ours	94.0	89.2	91.5
$k = 5$	NetVLAD	89.5	90.4	89.9
	Ours	90.9	89.4	90.1
$k = 10$	NetVLAD	90.0	90.5	90.2
	Ours	92.5	89.1	90.8

3) *KITTI Tracking Dataset*: The KITTI Tracking benchmark is a multi-object tracking dataset [43], thus we calculate the similarity of all object pairs in each frame pairs and use similar evaluation method with OTB and VOT. The overall performance on precision, recall, and F1-score are reported in Table III in which we still achieve a much higher performance

than NetVLAD. Their PRC are shown in Fig. 3c, in which we achieve a higher performance of 6.6%, 12.2%, and 14.7% for $k = 1, 5$, and 10 , respectively.

TABLE III: Object Matching on the KITTI Tracking dataset.

	Method	Precision	Recall	F1
$k = 1$	NetVLAD	82.6	84.4	83.5
	Ours	92.5	91.8	92.1
$k = 3$	NetVLAD	72.7	74.1	73.4
	Ours	86.5	83.4	84.9
$k = 5$	NetVLAD	68.6	68.8	68.7
	Ours	81.5	80.1	80.8
$k = 10$	NetVLAD	57.4	65.3	61.1
	Ours	73.7	72.7	73.2

C. Semantic Relocalization

To further verify its robustness, we apply the proposed method to semantic relocalization, which will be evaluated on the KITTI Odometry dataset [45]. For better evaluation, we select the sequences with significant loop closures, i.e., '00', '05', and '06'. Moreover, we mainly re-identify cars for relocalization, which is much more difficult than matching distinct objects. Although the overall performance of relocalization will be slightly harmed, such setting is able to verify the robustness of the object descriptor, as the cars on the road in KITTI datasets are very similar thus the performance on car re-identification is more convincing.

The overall performance is listed in Table IV, in which we can see that we achieve more reliable performance than NetVLAD for all sequences. Note that we don't perform assistant techniques such as geometric verification [2] to ensure that the improvements coming from the proposed object descriptor. We also present the recall curves in Fig. 5, in which we accept the top N pairs as a re-localization. It

TABLE IV: Semantic Relocalization on KITTI Odoemtry.

Sequence	Method	Precision	Recall	F1
00	NetVLAD	21.1	41.3	27.9
	Ours	50.8	86.9	64.1
05	NetVLAD	19.0	25.3	21.7
	Ours	43.7	48.0	45.7
06	NetVLAD	39.0	27.4	32.2
	Ours	71.4	63.2	67.1

can be seen that, $\forall N, N \in [1, 20]$, we able to achieve better performance with a large margin than NetVLAD for all sequences, which verifies the effectiveness of our method.

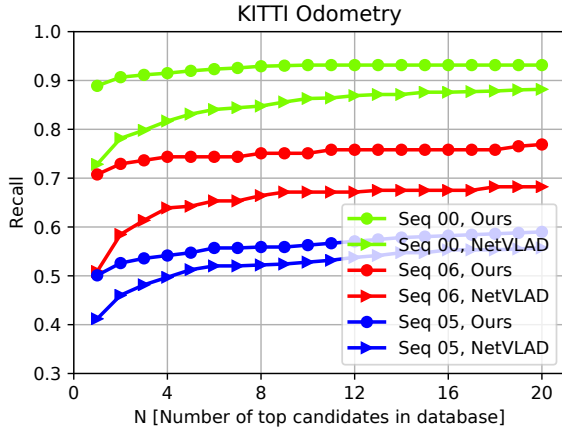


Fig. 5: The performance of semantic re-localization.

D. Live Demo

In this section, we present a live demo to demonstrate the generalization ability and robustness of the proposed method. We perform a very challenging object matching task shown in Fig. 1. In this demo, we use the pre-trained model mentioned in Section IV-B without any fine tuning. It can be seen that all the four objects including 1 rigid object and 3 non-rigid objects (human) are successfully identified. Moreover, it is robust to viewpoint (Obj 1 in (b) and (d)), scaling (Obj 3 and 4), occlusion (Obj 4), and even posture change (Obj 2 and 3). We argue that the robustness to object deformation is mainly because of that we adopt a key-point-based sparse encoding strategy, since the key-points (landmarks) often change less than appearance and the sparse encoding further makes it insensitive to the miss detected key-points.

V. ABLATION STUDY

We show the effects of the proposed sparsity module. All the statistics are obtained based on the COCO dataset.

A. Sparsity Analysis

In this section, we provide the sparsity analysis for the proposed object encoding method. The distribution of non-zero locations of the key-point features is shown in Fig. 6a, in which we can see that only 700-800 out of 2048 locations

are non-zeros. This verifies the objective of sparse loss in (4). The statistics of non-zero locations of the object descriptor is presented in Fig. 6b. As expected, the non-zero locations increase with the number of key-point detected in the object, which also verifies the objective of dense loss (5). Note that we expect to group similar key-points into similar locations as in (2a), thus the space of object descriptor will not be quickly used up by increasing the number of key-points.

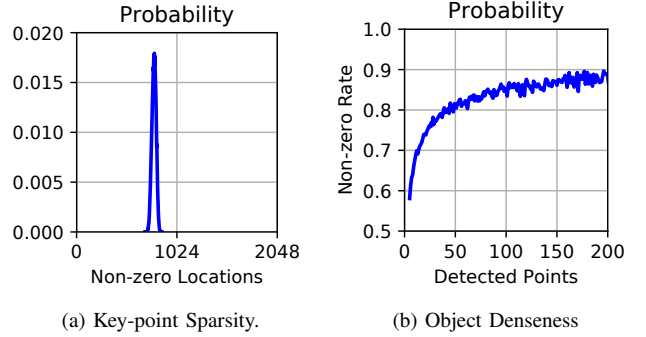


Fig. 6: The statistics of feature sparsity.

B. Efficiency

The operating efficiency is vital for robots, especially for low power robots such as unmanned aerial vehicles. This section presents the runtime of the proposed modules, which are listed in Table V. It can be seen that the sparsity layer only takes about 1 ms, which is much lower than the graph attention network used in this module. The overall running time is about 9.3 ms, which satisfies the real-time requirements of most robotic applications.

TABLE V: Runtime Analysis.

Module	Node Encoding	Graph	Sparsity	Overall
Time	0.847 ms	7.302 ms	1.131 ms	9.280 ms

VI. CONCLUSION

In this paper, we present a novel object encoding method, which can be used in many robotic tasks such as autonomous exploration and semantic relocalization. It is a plug-and-play module and can be easily adopted to any frameworks. To be robust to the number of key-points detected, we propose a sparse encoding method to ensure that each key-point can only affect a small part of the object descriptors, making the global descriptors robust in severe conditions such as viewpoint changes and object deformation. In the experiments, we show that it achieves superior performance in object matching and provides reliable semantic relocalization. We also show a live demo to demonstrate its robustness. We expect that this method will play an important role in robotic applications.

REFERENCES

- [1] C. Wang, W. Wang, Y. Qiu, Y. Hu, and S. Scherer, "Visual memorability for robotic interestingness via unsupervised online learning," in *European Conference on Computer Vision (ECCV)*, 2020.
- [2] H. Wang, C. Wang, and L. Xie, "Online visual place recognition via saliency re-identification," in *IEEE/RSJ International Conference on Intelligent Robots and Systems (IROS)*, 2020.
- [3] M.-P. Dubuisson and A. K. Jain, "A modified hausdorff distance for object matching," in *Proceedings of 12th international conference on pattern recognition*, vol. 1. IEEE, 1994, pp. 566–568.
- [4] R. Mur-Artal and J. D. Tardós, "Orb-slam2: An open-source slam system for monocular, stereo, and rgb-d cameras," *IEEE Transactions on Robotics*, vol. 33, no. 5, pp. 1255–1262, 2017.
- [5] D. DeTone, T. Malisiewicz, and A. Rabinovich, "Superpoint: Self-supervised interest point detection and description," in *Proceedings of the IEEE conference on computer vision and pattern recognition workshops*, 2018, pp. 224–236.
- [6] P.-E. Sarlin, D. DeTone, T. Malisiewicz, and A. Rabinovich, "Super-Glue: Learning feature matching with graph neural networks," in *CVPR*, 2020.
- [7] C. Wang, Y. Qiu, and S. Scherer, "Lifelong graph learning," *arXiv preprint arXiv:2009.00647*, 2020.
- [8] K. He, G. Gkioxari, P. Dollár, and R. Girshick, "Mask r-cnn," in *Proceedings of the IEEE international conference on computer vision*, 2017, pp. 2961–2969.
- [9] A. Glover, W. Maddern, M. Warren, S. Reid, M. Milford, and G. Wyeth, "Openfabmap: An open source toolbox for appearance-based loop closure detection," in *Robotics and automation (ICRA), 2012 IEEE international conference on*. IEEE, 2012, pp. 4730–4735.
- [10] H. Bay, T. Tuytelaars, and L. Van Gool, "Surf: Speeded up robust features," in *European conference on computer vision*. Springer, 2006, pp. 404–417.
- [11] D. Gálvez-López and J. D. Tardós, "Bags of binary words for fast place recognition in image sequences," *IEEE Transactions on Robotics*, vol. 28, no. 5, pp. 1188–1197, 2012.
- [12] E. Rublee, V. Rabaud, K. Konolige, and G. Bradski, "Orb: An efficient alternative to sift or surf," in *Computer Vision (ICCV), 2011 IEEE international conference on*. IEEE, 2011, pp. 2564–2571.
- [13] E. García-Fidalgo and A. Ortiz, "ibow-lcd: An appearance-based loop-closure detection approach using incremental bags of binary words," *IEEE Robotics and Automation Letters*, vol. 3, no. 4, pp. 3051–3057, 2018.
- [14] D. Schlegel and G. Grisetti, "Hbst: A hamming distance embedding binary search tree for visual place recognition," *arXiv preprint arXiv:1802.09261*, 2018.
- [15] P. L. N. Carrasco, F. Bonin-Font, and G. Oliver-Codina, "Global image signature for visual loop-closure detection," *Autonomous Robots*, vol. 40, no. 8, pp. 1403–1417, 2016.
- [16] M. Gehrig, E. Stumm, T. Hinzmann, and R. Siegwart, "Visual place recognition with probabilistic voting," in *2017 IEEE International Conference on Robotics and Automation (ICRA)*. IEEE, 2017, pp. 3192–3199.
- [17] S. Leutenegger, M. Chli, and R. Siegwart, "Brisk: Binary robust invariant scalable keypoints," in *2011 IEEE international conference on computer vision (ICCV)*. Ieee, 2011, pp. 2548–2555.
- [18] K. A. Tsintotas, L. Bampis, and A. Gasteratos, "Assigning visual words to places for loop closure detection," in *2018 IEEE International Conference on Robotics and Automation (ICRA)*. IEEE, 2018, pp. 1–7.
- [19] B. Fritzke, "A growing neural gas network learns topologies," in *Advances in neural information processing systems*, 1995, pp. 625–632.
- [20] E. Stumm, C. Mei, S. Lacroix, J. Nieto, M. Hutter, and R. Siegwart, "Robust visual place recognition with graph kernels," in *Proceedings of the IEEE Conference on Computer Vision and Pattern Recognition*, 2016, pp. 4535–4544.
- [21] D. Schlegel and G. Grisetti, "Adding cues to binary feature descriptors for visual place recognition," in *2019 International Conference on Robotics and Automation (ICRA)*. IEEE, 2019, pp. 5488–5494.
- [22] C. Wang, J. Yang, L. Xie, and J. Yuan, "Kervolutional neural networks," in *The IEEE Conference on Computer Vision and Pattern Recognition (CVPR)*, 2019, pp. 31–40.
- [23] Z. Chen, A. Jacobson, N. Sünderhauf, B. Upcroft, L. Liu, C. Shen, I. Reid, and M. Milford, "Deep learning features at scale for visual place recognition," in *2017 IEEE International Conference on Robotics and Automation (ICRA)*. IEEE, 2017, pp. 3223–3230.
- [24] R. Arandjelovic, P. Gronat, A. Torii, T. Pajdla, and J. Sivic, "Netvlad: Cnn architecture for weakly supervised place recognition," in *Proceedings of the IEEE conference on computer vision and pattern recognition*, 2016, pp. 5297–5307.
- [25] S. Hausler, A. Jacobson, and M. Milford, "Multi-process fusion: Visual place recognition using multiple image processing methods," *IEEE Robotics and Automation Letters*, vol. 4, no. 2, pp. 1924–1931, 2019.
- [26] N. Dalal and B. Triggs, "Histograms of oriented gradients for human detection," in *Proceedings of the IEEE Computer Society Conference on Computer Vision and Pattern Recognition (CVPR)*, 2005.
- [27] H. F. Zaki, F. Shafait, and A. Mian, "Convolutional hypercube pyramid for accurate rgb-d object category and instance recognition," in *2016 IEEE International Conference on Robotics and Automation (ICRA)*. IEEE, 2016, pp. 1685–1692.
- [28] M. Schwarz, H. Schulz, and S. Behnke, "Rgb-d object recognition and pose estimation based on pre-trained convolutional neural network features," in *2015 IEEE international conference on robotics and automation (ICRA)*. IEEE, 2015, pp. 1329–1335.
- [29] H. F. Zaki, F. Shafait, and A. Mian, "Viewpoint invariant semantic object and scene categorization with rgb-d sensors," *Autonomous Robots*, vol. 43, no. 4, pp. 1005–1022, 2019.
- [30] M. J. Tarr and W. G. Hayward, "The concurrent encoding of viewpoint-invariant and viewpoint-dependent information in visual object recognition," *Visual Cognition*, vol. 25, no. 1-3, pp. 100–121, 2017.
- [31] K. Simonyan and A. Zisserman, "Very deep convolutional networks for large-scale image recognition," *arXiv:1409.1556*, 2014.
- [32] P. Veličković, G. Cucurull, A. Casanova, A. Romero, P. Liò, and Y. Bengio, "Graph Attention Networks," *International Conference on Learning Representations (ICLR)*, 2018.
- [33] D. G. Lowe, "Distinctive image features from scale-invariant keypoints," *International journal of computer vision*, vol. 60, no. 2, pp. 91–110, 2004.
- [34] H. Lee, A. Battle, R. Raina, and A. Y. Ng, "Efficient sparse coding algorithms," in *Advances in neural information processing systems*. Citeseer, 2007, pp. 801–808.
- [35] Y. Gwon, M. Cha, and H. Kung, "Deep sparse-coded network (dsn)," in *2016 23rd International Conference on Pattern Recognition (ICPR)*. IEEE, 2016, pp. 2610–2615.
- [36] X. Liu, W. Li, J. Huo, L. Yao, and Y. Gao, "Layerwise sparse coding for pruned deep neural networks with extreme compression ratio," in *Proceedings of the AAAI Conference on Artificial Intelligence*, vol. 34, no. 04, 2020, pp. 4900–4907.
- [37] T.-Y. Lin, M. Maire, S. Belongie, J. Hays, P. Perona, D. Ramanan, P. Dollár, and C. L. Zitnick, "Microsoft coco: Common objects in context," in *European conference on computer vision*. Springer, 2014, pp. 740–755.
- [38] G. Hinton, N. Srivastava, and K. Swersky, "Neural networks for machine learning lecture 6a overview of mini-batch gradient descent," *Cited on*, vol. 14, no. 8, 2012.
- [39] P.-E. Sarlin, C. Cadena, R. Siegwart, and M. Dymczyk, "From coarse to fine: Robust hierarchical localization at large scale," in *Proceedings of the IEEE/CVF Conference on Computer Vision and Pattern Recognition*, 2019, pp. 12716–12725.
- [40] Z. Liu, S. Zhou, C. Suo, P. Yin, W. Chen, H. Wang, H. Li, and Y.-H. Liu, "Lpd-net: 3d point cloud learning for large-scale place recognition and environment analysis," in *Proceedings of the IEEE/CVF International Conference on Computer Vision (ICCV)*, October 2019.
- [41] Y. Wu, J. Lim, and M.-H. Yang, "Online object tracking: A benchmark," in *IEEE Conference on Computer Vision and Pattern Recognition (CVPR)*, 2013.
- [42] M. Kristan, J. Matas, A. Leonardis, T. Vojir, R. Pflugfelder, G. Fernandez, G. Nebel, F. Porikli, and L. Čehovin, "A novel performance evaluation methodology for single-target trackers," *IEEE Transactions on Pattern Analysis and Machine Intelligence*, vol. 38, no. 11, pp. 2137–2155, Nov 2016.
- [43] J. Luiten, A. Osep, P. Dendorfer, P. Torr, A. Geiger, L. Leal-Taixe, and B. Leibe, "Hota: A higher order metric for evaluating multi-object tracking," *International Journal of Computer Vision (IJCV)*, 2020.
- [44] C. Wang, L. Zhang, L. Xie, and J. Yuan, "Kernel cross-correlator," in *Thirty-Second AAAI Conference on Artificial Intelligence (AAAI)*, 2018, pp. 4179–4186.
- [45] A. Geiger, P. Lenz, and R. Urtasun, "Are we ready for autonomous driving? the kitti vision benchmark suite," in *Conference on Computer Vision and Pattern Recognition (CVPR)*, 2012.